RESEARCH ARTICLE

Editor's Choice

ADVANCED
MATERIALS
INTERFACES
Open Access

www.advmatinterfaces.de

Crystalline Silicon Photocathode with Tapered Microwire Arrays Achieving a High Current Density of 41.7 mA cm^{-2}

Wonjoo Jin, Youri Lee, Changhwan Shin, Jeonghwan Park, Ji-Wook Jang,* and Kwanyong Seo*

To design a high-efficiency crystalline silicon (*c*-Si) photocathode, the photovoltage and photocurrent generated by the device must be maximized because these factors directly affect the hydrogen evolution reaction (HER). In this study, a *c*-Si *p–n* junction is used to enhance the photovoltage of the *c*-Si photocathode, and a tapered microwire array structure is introduced to increase the photocurrent. When tapered microwire arrays are employed on the front surface of the *c*-Si photocathode, a current density of ≈41.7 mA cm^{-2} is achieved at 0 V_{RHE} (reversible hydrogen electrode); this current density is the highest among all reported photocathodes including *c*-Si, approaching the theoretical maximum value for *c*-Si. Furthermore, a Ni foil/Pt catalyst is introduced on the opposite side of the incident light, simultaneously serving as an electrocatalyst to reduce side reactions in the HER and encapsulation layer to prevent *c*-Si from contacting the electrolyte. Thus, a stable device is developed using *c*-Si photoelectrochemical cells that have an efficiency exceeding 97% for >1000 h.

1. Introduction

Photoelectrochemical (PEC) cells are being extensively investigated for water splitting because they can directly convert solar energy into clean, sustainable hydrogen fuel.[1,2] Since Fujishima and Honda reported the design of a PEC cell using TiO$_2$ in 1972,

W. Jin, Y. Lee, C. Shin, J. Park, J.-W. Jang, K. Seo
School of Energy and Chemical Engineering
Ulsan National Institute of Science and Technology (UNIST)
Ulju-gun, Ulsan 44919, Republic of Korea
E-mail: jiwjang@unist.ac.kr; kseo@unist.ac.kr

J.-W. Jang
Emergent Hydrogen Technology R&D Center
Ulsan National Institute of Science and Technology (UNIST)
Ulju-gun, Ulsan 44919, Republic of Korea

J.-W. Jang, K. Seo
Graduate School of Carbon Neutrality
Ulsan National Institute of Science and Technology (UNIST)
Ulju-gun, Ulsan 44919, Republic of Korea

The ORCID identification number(s) for the author(s) of this article can be found under https://doi.org/10.1002/admi.202400178

various semiconductor-based PEC studies have been conducted on materials such as Fe$_2$O$_3$, WO$_3$, BiVO$_4$, Ta$_3$N$_5$, SrTiO$_3$, Cu$_2$O, crystalline silicon (*c*-Si), and amorphous silicon (*a*-Si).[3–8] Among these materials, *c*-Si is considered a particularly promising material for PEC applications owing to its abundant availability, low cost, established production technology, and narrow band gap (1.1 eV), which facilitates the efficient absorption of sunlight in the visible spectrum.[9–14] The theoretical maximum photocurrent of *c*-Si photoelectrode has been reported to approach 44 mA cm^{-2}, exceeding the theoretical maximum values of other materials such as TiO$_2$ (1.8 mA cm^{-2}), BiVO$_4$ (7.5 mA cm^{-2}), Fe$_2$O$_3$ (10.7 mA cm^{-2}), and Cu$_2$O (12.5 mA cm^{-2}).[15—17] However, *c*-Si photoelectrodes are unstable, particularly under alkaline conditions.[18] Therefore, a high photocurrent and stable c-Si photoelectrode are necessary for its practical application.

Various studies have been conducted to minimize light reflection and maximize absorption by applying nano- and microstructures on the front surface of the device. Among various surface structures, microwire arrays employed on top of *c*-Si can increase the current density, approaching a theoretical maximum of 44 mA cm^{-2}.[17,19–23] Lewis et al. reported *c*-Si microwire structures in conjunction with a Pt catalyst to achieve a photocurrent density of 15 mA cm^{-2}.[24] Huskens et al. employed *c*-Si silicon microwire structures together with a Ni–Mo catalyst to achieve a photocurrent density of 35.5 mA cm^{-2}.[25] In addition, a hydrogen evolution reaction (HER) electrocatalyst has been deposited on top of a *c*-Si photocathode to obtain an efficient HER, and the *c*-Si microwire surface was passivated to prevent electrolyte permeation. However, the HER cannot efficiently occur with a small amount of the HER electrocatalyst, and the stability of the *c*-Si photocathode is reduced because the entire surface of the *c*-Si microwire cannot be effectively covered. Conversely, loading a large amount of HER electrocatalyst on the *c*-Si photocathode blocks light, thereby reducing the photocurrent density. Consequently, the reported photocurrent density values of *c*-Si microwire photocathodes do not approach the theoretical maximum of 44 mA cm^{-2}, and the devices have insufficient stability.[24,25]

In this study, a high-performance *c*-Si tapered microwire (TMW) photocathode was fabricated using a *c*-Si *p–n* junction

**ADVANCED
SCIENCE NEWS**

www.advancedsciencenews.com

**ADVANCED
MATERIALS
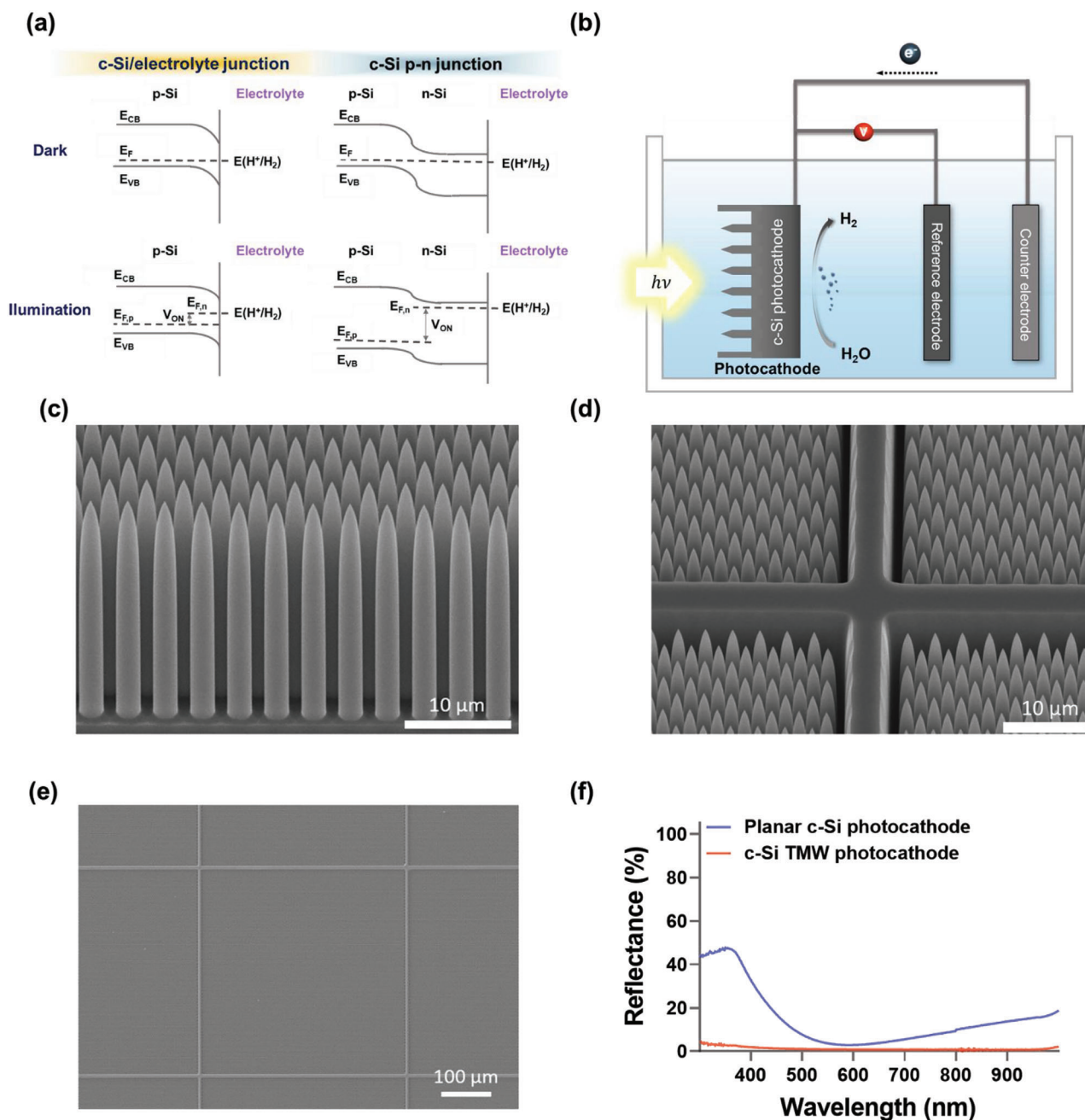INTERFACES**
Open Access

www.advmatinterfaces.de

Figure 1. Schematic of the c-Si tapered microwire (TMW) photocathode and its performance. a) Energy band alignment of *c*-Si/electrolyte and *c*-Si p–n junction under illumination and in the dark. b) Schematic illustration of *c*-Si TMW photocathodes. c) Tilted view of a scanning electron microscopy (SEM) image. d) high-magnification top-view and e) low-magnification top-view SEM images. f) Reflectance spectra of planar *c*-Si and *c*-Si TMW photocathodes.

and tapered microwire arrays on the front surface of the device to maximize the optical performance. Additionally, a Pt/Ni catalyst was used on the opposite side of the TMW array structure to simultaneously serve as an electrocatalyst and an encapsulation layer for the *c*-Si photocathode, thereby providing high stability and efficiency. Consequently, a record-high photocurrent density of 41.7 mA cm^{-2} was achieved at 0 V$_{RHE}$ (reversible hydrogen electrode) with a favorable onset potential of 0.6 V$_{RHE}$. Furthermore, this high performance was maintained for 1000 h with

less than a 3% decrease in performance. These results demonstrate that the proposed photocathode had the highest photocurrent density and stability among all *c*-Si photocathodes reported thus far.

2. Results and Discussion

c-Si has been extensively studied as a suitable photocathode material for the HER because its conduction band edge position
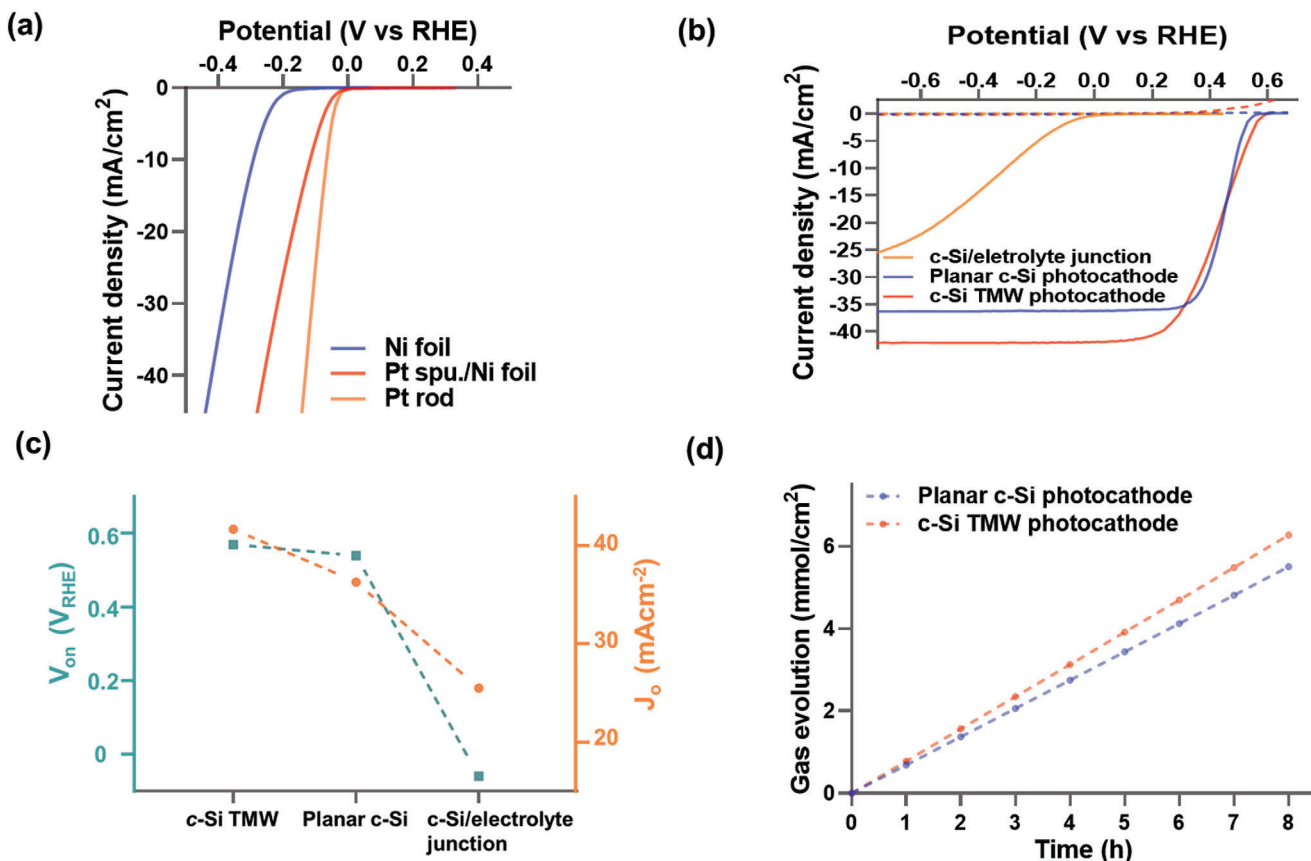
2400178 (2 of 6)

**ADVANCED
SCIENCE NEWS**

www.advancedsciencenews.com

**ADVANCED
MATERIALS
INTERFACES**

www.advmatinterfaces.de

Figure 2. Properties of the *c*-Si TMW photocathode. a) Hydrogen evolution reaction *J–V* curves of Ni foil and Pt sputtered on Ni foil versus a reversible hydrogen electrode (RHE). b) Linear sweep voltammetry (LSV) curves of *c*-Si electrolyte junction and *c*-Si p–n junction (planar *c*-Si and *c*-Si TMW photocathodes). c) Comparison of onset potential (V_{ON}) and photocurrent density at 0 V_{RHE} (J_0). d) Evolution of hydrogen gas during the chronoamperometry test at 0 V_{RHE}. All photoelectrocatalytic performances were measured under one sun illumination (AM 1.5 G) in 0.5 M H_2SO_4.

is more negative than the potential required for the HER.[12–14,24,26,27] However, *c*-Si exhibits a low PEC efficiency owing to the relatively low photovoltage (≈0.2 V) formed at the *c*-Si/electrolyte heterojunction.[24,28–30] To enhance the photovoltage, a *c*-Si p–n junction has been recently investigated as an alternative to the *c*-Si/electrolyte heterojunction.[14,26–28,31] The photovoltage of the *c*-Si p–n junction is relatively high (>0.6 V) compared to that of the *c*-Si/electrolyte heterojunction owing to the energy difference between quasi-Fermi levels that are formed through Fermi-level splitting in the p–n junction under light illumination; thus, relatively high-voltage photocathodes have been reported.[14,26,27] As shown in the energy diagram in **Figure** 1a, the *c*-Si/electrolyte junction exhibits a low photovoltage (≈0.2 V) because *c*-Si directly forms a heterojunction with the electrolyte. In contrast, when using a *c*-Si p–n junction, a high photovoltage (>0.6 V) is observed because of the energy difference between the quasi-Fermi levels formed through Fermi-level splitting. In addition to the p–n junction, TMW arrays were placed on top of *c*-Si to maximize light absorption by *c*-Si; to minimize optical hindrance, the electrocatalyst was placed on the rear side of *c*-Si (Figure 1b). The TMW arrays can effectively maximize the absorption of *c*-Si because the effective refractive index (*n*) gradually increases from air (*n* = 1) to *c*-Si (*n* = 4). This gradual increase in *n* enables the effective reduction of reflection in the wavelength

range of 300—1000 nm, which can be absorbed by *c*-Si. The *c*-Si TMW photocathode was fabricated as follows: Initially, the *c*-Si microwire array was fabricated via photolithography and deep reactive-ion etching. Subsequently, a tapered structure was formed using an isotropic Si etchant in a wet etching process. The detailed fabrication process is described in the Experimental section and Figure S1 (Supporting Information). As shown in the scanning electron microscopy (SEM) image (Figure 1c), the dimensions of the fabricated TMW array were: diameter = 2 μm, length = 20 μm, and spacing = 1 μm. Particularly, the TMW array was fabricated in an embedded form to ensure high mechanical stability, which facilitated the reproducible fabrication of the photocathode with TMW arrays (Figure 1d,e). As visually confirmed in the optical photograph in Figure S2 (Supporting Information), the *c*-Si TMW surface appears blacker than planar *c*-Si with SiN_x as an additional anti-reflection coating (ARC) layer, demonstrating that the surface reflection of the *c*-Si TMW specimen is substantially reduced. The optical characteristics of the fabricated *c*-Si TMW arrays were analyzed using an ultraviolet–visible–near-infrared (UV–vis–NIR) spectrophotometer. The average reflectance of *c*-Si TMW arrays was extremely low (1.2%) across the entire range of 300—1000 nm that *c*-Si can absorb light compared to that (14.8%) of planar *c*-Si with SiN_x (Figure 1f).
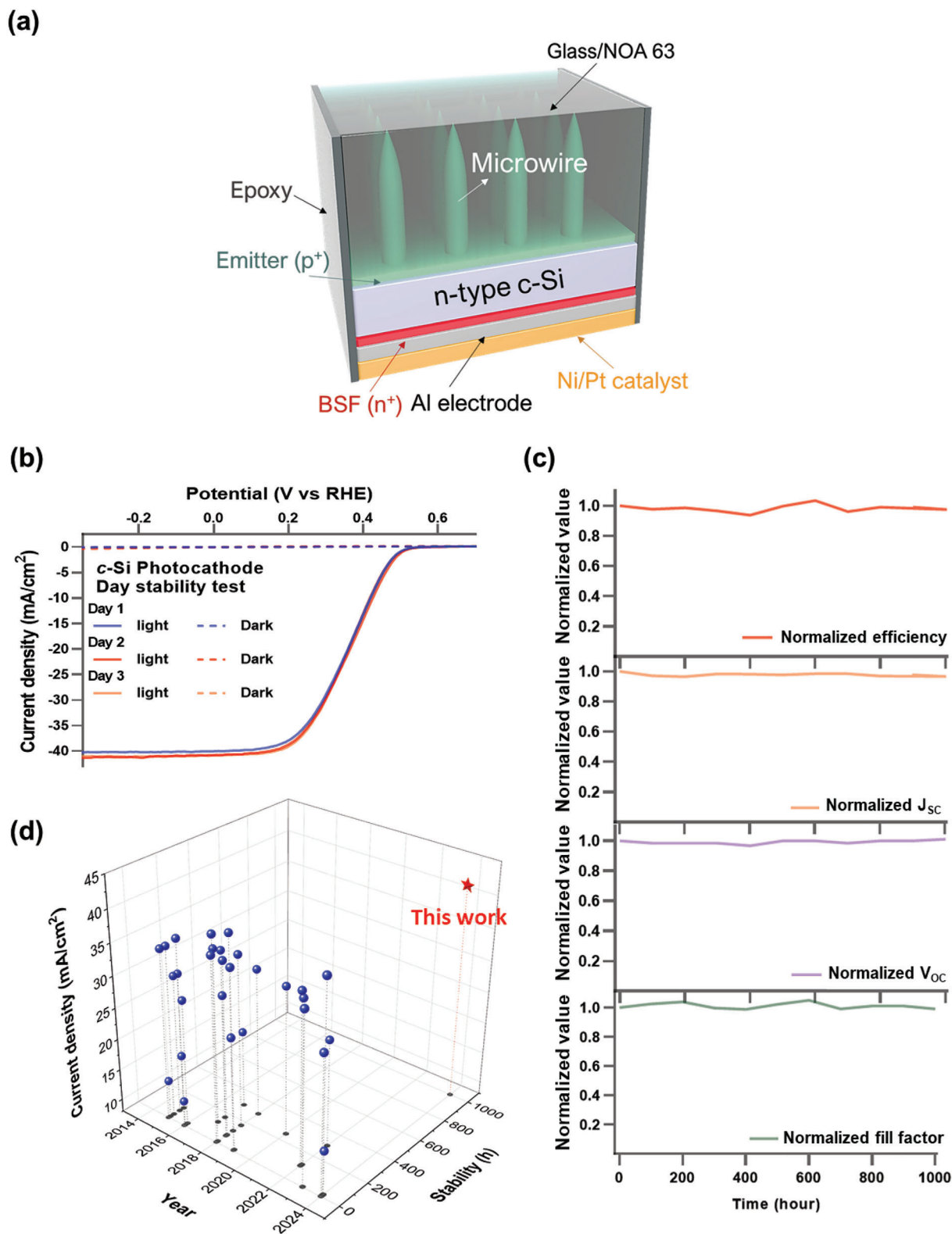
ADVANCED
SCIENCE NEWS

www.advancedsciencenews.com

ADVANCED
MATERIALS
INTERFACES
Open Access

www.advmatinterfaces.de

Figure 3. Stability of the *c*-Si TMW photocathode. a) Schematic of the *c*-Si TMW photocathode. b) LSV curves of the *c*-Si TMW photocathode for long-term durations c) Photovoltaic performance measurements in the long-term periods. d) Historical trends in the reported *c*-Si photocathode photocurrent densities and stability. All photoelectrochemical performances were measured under one sun illumination (AM 1.5 G) in 0.5 M H_2SO_4.

Currently, the catalyst with the highest performance for the HER is Pt.[32] However, Pt is an expensive noble metal, which is an economic obstacle to its use. Therefore, to minimize the use of expensive Pt catalysts, a 10-nm-thick Pt layer was sputtered on top of Ni instead of using pure Pt as the catalyst. The electrochemical measurements of Ni and Pt/Ni are shown in **Figure 2a**, and V_{ON} of Pt/Ni (−0.04 V) is similar to that of Pt alone (−0.03 V) and considerably higher than that of Ni alone (−0.21 V).

To evaluate the performance of the *c*-Si TMW photocathode, a current–voltage (*J–V*) curve was obtained using linear sweep voltammetry (LSV) (Figure 2b). The *c*-Si TMW photocathode exhibited a current density of 41.7 mA cm^{-2}, ≈16% higher than that of the planar *c*-Si photocathode with an ARC layer (36.1 mA cm^{-2}). This improvement is primarily attributed to the low reflectance of the *c*-Si TMW photocathode (Figure 1f), and it is further supported by the *J–V* curve of the *c*-Si *p–n* junction-based solar cell (Figure S3, Supporting Information). Moreover, as depicted in the energy diagram (Figure 1a) and consistent with the abovementioned findings, the *c*-Si *p–n* junction (both planar *c*-Si and *c*-Si TMW photocathode) exhibited a higher V_{ON} (≈0.6 V) than that of the conventional *c*-Si/electrolyte heterojunction. Figure 2c provides a distinctive comparison of V_{ON} and saturation photocurrent density at 0 V_{RHE} (J_0) from the LSV curve for the various *c*-Si photocathodes presented in Figure 2b. Both the *p–n* junction-based planar *c*-Si and *c*-Si TMW photocathodes demonstrate V_{ON} values of ≈0.6 V, which is higher than that of the *c*-Si/electrolyte junction (−0.1 V). Additionally, J_0 of the *c*-Si TMW photocathode is higher than that of the planar *p–n* junction *c*-Si photocathode and *c*-Si/electrolyte junction. When measured under 0 V_{RHE} conditions using gas chromatography, the *c*-Si TMW photocathode exhibited a hydrogen production rate of 0.78 mmol cm^{-2} h^{-1}, ≈15% higher than that of the planar *c*-Si photocathode (Figure 2d), which is consistent with the current density presented in Figure 2b,c.

The *c*-Si TMW photocathode was subjected to a long-term stability test to evaluate its encapsulation effectiveness. The schematic of the *c*-Si TMW photocathode provides a detailed view of the device structure (**Figure 3a**). Initially, we arranged the *c*-Si photocathode with TMW arrays facing a glass substrate using optical glue (NOA 63). During this process, the durability of the TMW arrays on *c*-Si was confirmed without any mechanical issues, owing to the embedded structure (Figure 1d). Subsequently, we affixed Pt-sputtered Ni foil with Ag paste on the rear side of the *c*-Si photocathode to protect the entire rear surface from the electrolyte. Finally, to completely prevent any chemical reactions of *c*-Si with the electrolyte, the side area of the device was encapsulated with an epoxy resin. Figure 3a depicts a schematic of the *c*-Si TMW encapsulated photocathode. This design intrinsically eliminates direct contact between *c*-Si and the electrolyte, markedly enhancing the stability of the *c*-Si TMW photocathode. Repeated LSV measurements were conducted for 72 h at 24-h intervals to confirm that V_{ON} and J_0 remained nearly unchanged; these parameters retained ≈97% of their initial values (Figure 3b). Furthermore, we continuously measured the photovoltaic performance of the *c*-Si TMW photocathode, including short-circuit current density (J_{SC}), open-circuit voltage (V_{OC}), fill factor (*FF*), and overall efficiency, for over 1000 h. All photovoltaic factors were stable within 97% of their initial values under AM 1.5 G illumination (Figure 3c). Particularly, our device

exhibited an extremely high long-term stability (1000 h) and the highest photocurrent (41.7 mA cm^{-2}) compared to those reported for other *c*-Si photocathodes (Figure 3d, Table S1, Supporting Information).[18,28,31,33–57]

3. Conclusion

We successfully demonstrated a high-efficiency *c*-Si TMW photocathode employing a *c*-Si *p–n* junction, which addressed the challenge of low photovoltage observed in conventional *c*-Si/electrolyte heterojunctions. In addition, the TMW structure on the front surface of *c*-Si maximized the light absorption of the photocathode, substantially enhancing the photocurrent density. The current density at 0 V_{RHE} of the *c*-Si TMW photocathode reached 41.7 mA cm^{-2}, which is the highest value among all photocathodes reported thus far, including *c*-Si photocathodes. Furthermore, we confirmed that Ni foil can serve as both a catalyst and an encapsulation layer on the rear surface of the *c*-Si photocathode. Consequently, a *c*-Si TMW photocathode with a high photocurrent density (41.7 mA cm^{-2}) and long-term stability (1000 h) was obtained.

Supporting Information

Supporting Information is available from the Wiley Online Library or from the author.

Conflict of interest

The authors declare no conflict of interest.

Data Availability Statement

Research data are not shared.

**ADVANCED
SCIENCE NEWS**

www.advancedsciencenews.com

**ADVANCED
MATERIALS
INTERFACES**
Open Access

www.advmatinterfaces.de

[1] L. Barreto, A. Makihira, K. Riahi, *Int. J. Hydrogen Energy* **2003**, *28*, 267.

[2] S. A. Bonke, M. Wiechen, D. R. MacFarlane, L. Spiccia, *Energy Environ. Sci.* **2015**, *8*, 2791.

[3] A. Fujishima, K. Honda, *Nature* **1972**, *238*, 37.

[4] S. Kawasaki, R. Takahashi, T. Yamamoto, M. Kobayashi, H. Kumigashira, J. Yoshinobu, F. Komori, A. Kudo, M. Lippmaa, *Nat. Commun.* **2016**, *7*, 11818.

[5] Y. H. Ng, A. Iwase, A. Kudo, R. Amal, *J. Phys. Chem. Lett.* **2010**, *1*, 2607.

[6] J. Su, L. Guo, N. Bao, C. A. Grimes, *Nano Lett.* **2011**, *11*, 1928.

[7] J. Yang, C. Bao, T. Yu, Y. Hu, W. Luo, W. Zhu, G. Fu, Z. Li, H. Gao, F. Li, Z. Zou, *ACS Appl. Mater. Interfaces* **2015**, *7*, 26482.

[8] C. Zhen, L. Wang, G. Liu, G. Q. M. Lu, H. M. Cheng, *Chem. Commun.* **2013**, *49*, 3019.

[9] Y. Yu, Z. Zhang, X. Yin, A. Kvit, Q. Liao, Z. Kang, X. Yan, Y. Zhang, X. Wang, *Nat. Energy* **2017**, *2*, 17045.

[10] K. Sun, S. Shen, Y. Liang, P. E. Burrows, S. S. Mao, D. Wang, *Chem. Rev.* **2014**, *114*, 8662.

[11] A. G. Scheuermann, J. P. Lawrence, K. W. Kemp, T. Ito, A. Walsh, C. E. Chidsey, P. K. Hurley, P. C. McIntyre, *Nat. Mater.* **2016**, *15*, 99.

[12] E. L. Warren, H. A. Atwater, N. S. Lewis, *J. Phys. Chem. C* **2014**, *118*, 747.

[13] M. R. Shaner, J. R. McKone, H. B. Gray, N. S. Lewis, *Energy Environ. Sci.* **2015**, *8*, 2977.

[14] S. Wang, T. Wang, B. Liu, H. Li, S. Feng, J. Gong, *Natl. Sci. Rev.* **2021**, *8*, nwaa293.

[15] S. Hu, C. Xiang, S. Haussener, A. D. Berger, N. S. Lewis, *Energy Environ. Sci.* **2013**, *6*, 2984.

[16] T. J. Jacobsson, V. Fjällström, M. Edoff, T. Edvinsson, *Sol. Energy Mater. Sol. Cells* **2015**, *138*, 86.

[17] C. Liu, N. P. Dasgupta, P. Yang, *Chem. Mater.* **2014**, *26*, 415.

[18] W. Vijselaar, R. M. Tiggelaar, H. Gardeniers, J. Huskens, *ACS Energy Lett.* **2018**, *3*, 1086.

[19] H. D. Um, K. Lee, I. Hwang, J. Park, D. Choi, N. Kim, H. Kim, K. Seo, *J. Mater. Chem. A* **2020**, *8*, 5395.

[20] H. D. Um, I. Hwang, D. Choi, K. Seo, *Acc. Mater. Res.* **2021**, *2*, 701.

[21] I. Hwang, H. D. Um, B. S. Kim, M. Wober, K. Seo, *Energy Environ. Sci.* **2018**, *11*, 641.

[22] D. Choi, K. Seo, *Adv. Energy Mater.* **2021**, *11*, 2003707.

[23] N. Kim, D. Choi, H. Kim, H. D. Um, K. Seo, *ACS Nano* **2021**, *15*, 14756.

[24] S. W. Boettcher, E. L. Warren, M. C. Putnam, E. A. Santori, D. Turner-Evans, M. D. Kelzenberg, M. G. Walter, J. R. McKone, B. S. Brunschwig, H. A. Atwater, N. S. Lewis, *J. Am. Chem. Soc.* **2011**, *133*, 1216.

[25] W. Vijselaar, P. Westerik, J. Veerbeek, R. M. Tiggelaar, E. Berenschot, N. R. Tas, H. Gardeniers, J. Huskens, *Nat. Energy* **2018**, *3*, 185.

[26] E. L. Warren, J. R. McKone, H. A. Atwater, H. B. Gray, N. S. Lewis, *Energy Environ. Sci.* **2012**, *5*, 9653.

[27] R. Fan, W. Dong, L. Fang, F. Zheng, M. Shen, *J. Mater. Chem. A* **2017**, *5*, 18744.

[28] Z. Yin, R. Fan, G. Huang, M. Shen, *Chem. Commun.* **2018**, *54*, 543.

[29] R. N. Dominey, N. S. Lewis, J. A. Bruce, D. C. Bookbinder, M. S. Wrighton, *J. Am. Chem. Soc.* **1982**, *104*, 467.

[30] I. Lombardi, S. Marchionna, G. Zangari, S. Pizzini, *Langmuir* **2007**, *23*, 12413.

[31] H. Li, B. Liu, S. Feng, H. Li, T. Wang, J. Gong, *J. Mater. Chem. A* **2020**, *8*, 224.

[32] J. N. Hansen, H. Prats, K. K. Toudahl, N. Mørch Secher, K. Chan, J. Kibsgaard, I. Chorkendorff, *ACS Energy Lett.* **2021**, *6*, 1175.

[33] A. Alarawi, V. Ramalingam, H. C. Fu, P. Varadhan, R. Yang, J. H. He, *Opt. Express* **2019**, *27*, A352.

[34] Q. Jia, C. Yu, W. Liu, G. Zheng, C. Lei, L. Lei, X. Zhang, *J. Energy Chem.* **2019**, *30*, 101.

[35] R. Fan, C. Tang, Y. Xin, X. Su, X. Wang, M. Shen, *Appl. Phys. Lett.* **2016**, 109.

[36] R. Fan, J. Min, Y. Li, X. Su, S. Zou, X. Wang, M. Shen, *Appl. Phys. Lett.* **2015**, 106.

[37] Y. Wan, S. K. Karuturi, C. Samundsett, J. Bullock, M. Hettick, D. Yan, J. Peng, P. R. Narangari, S. Mokkapati, H. H. Tan, *ACS Energy Lett.* **2018**, *3*, 125.

[38] C. Ros, T. Andreu, M. D. Hernández-Alonso, G. Penelas-Perez, J. Arbiol, J. R. Morante, *ACS Appl. Mater. Interfaces* **2017**, *9*, 17932.

[39] R. Fan, G. Huang, Y. Wang, Z. Mi, M. Shen, *Appl. Catal., B* **2018**, *237*, 158.

[40] G. Huang, J. Mao, R. Fan, Z. Yin, X. Wu, J. Jie, Z. Kang, M. Shen, *Appl. Phys. Lett.* **2018**, *112*.

[41] C. W. Roske, E. J. Popczun, B. Seger, C. G. Read, T. Pedersen, O. Hansen, P. C. Vesborg, B. S. Brunschwig, R. E. Schaak, I. Chorkendorff, *J. Phys. Chem. Lett.* **2015**, *6*, 1679.

[42] F. Chen, Q. Zhu, Y. Wang, W. Cui, X. Su, Y. Li, *ACS Appl. Mater. Interfaces* **2016**, *8*, 31025.

[43] S. Vanka, E. Arca, S. Cheng, K. Sun, G. A. Botton, G. Teeter, Z. Mi, *Nano Lett.* **2018**, *18*, 6530.

[44] R. Fan, W. Dong, L. Fang, F. Zheng, X. Su, S. Zou, J. Huang, X. Wang, M. Shen, *Appl. Phys. Lett.* **2015**, *106*.

[45] B. Zhou, X. Kong, S. Vanka, S. Chu, P. Ghamari, Y. Wang, N. Pant, I. Shih, H. Guo, Z. Mi, *Nat. Commun.* **2018**, *9*, 3759.

[46] L. Ji, M. D. McDaniel, S. Wang, A. B. Posadas, X. Li, H. Huang, J. C. Lee, A. A. Demkov, A. J. Bard, J. G. Ekerdt, *Nat. Nanotechnol.* **2015**, *10*, 84.

[47] M. Cabán-Acevedo, M. L. Stone, J. Schmidt, J. G. Thomas, Q. Ding, H. C. Chang, M. L. Tsai, J. H. He, S. Jin, *Nat. Mater.* **2015**, *14*, 1245.

[48] R. Fan, J. Mao, Z. Yin, J. Jie, W. Dong, L. Fang, F. Zheng, M. Shen, *ACS Appl. Mater. Interfaces* **2017**, *9*, 6123.

[49] Y. Yang, M. Wang, P. Zhang, W. Wang, H. Han, L. Sun, *ACS Appl. Mater. Interfaces* **2016**, *8*, 30143.

[50] H. Zhang, Q. Ding, D. He, H. Liu, W. Liu, Z. Li, B. Yang, X. Zhang, L. Lei, S. Jin, *Energy Environ. Sci.* **2016**, *9*, 3113.

[51] S. Li, H. Lin, G. Yang, X. Ren, S. Luo, J. Ye, *Chem. Eng. J.* **2023**, *455*, 140898.

[52] H. Zhang, S. Li, J. Xu, X. Sun, J. Xia, G. She, J. Yu, C. Ru, J. Luo, X. Meng, L. Mu, W. Shi, *Small*.

[53] C. Ding, C. Li, W. Xiao, Q. Chen, Y. Li, J. He, C. Li, *Int. J. Hydrogen Energy* **2024**, *66*, 40.

[54] C. Chen, Y. Wang, C. Nie, J. Shen, Z. Wei, S. Zou, X. Su, R. Fan, Y. Peng, M. Shen, *Adv. Energy Mater.* **2022**, *12*, 2102865.

[55] S. Li, H. Lin, G. Yang, X. Ren, S. Luo, X.-s. Wang, Z. Chang, J. Ye, *Appl. Catal., B* **2022**, *304*, 120954.

[56] B. Wu, T. Wang, B. Liu, H. Li, Y. Wang, S. Wang, L. Zhang, S. Jiang, C. Pei, J. Gong, *Nat. Commun.* **2022**, *13*, 4460.

[57] Y. Hu, W. Zhou, W. Gong, C. Gao, S. Shen, T. Kong, Y. Xiong, *Angew. Chem., Int. Ed.* **2024**.

2400178 (6 of 6)